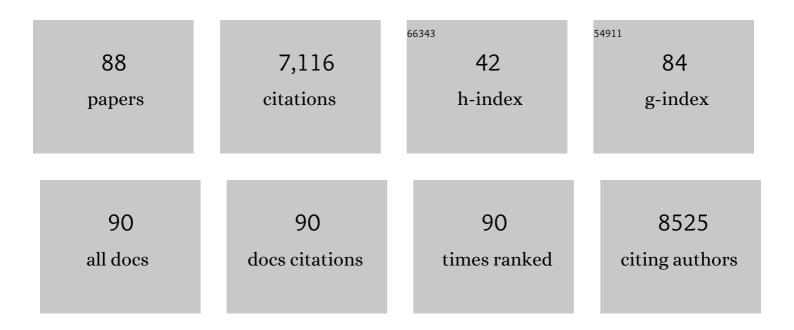
List of Publications by Year in descending order

Source: https://exaly.com/author-pdf/4782149/publications.pdf Version: 2024-02-01



#	Article	IF	CITATIONS
1	Nitrogen-Doped Titanium Dioxide as Visible-Light-Sensitive Photocatalyst: Designs, Developments, and Prospects. Chemical Reviews, 2014, 114, 9824-9852.	47.7	1,086
2	Band-Gap Narrowing of Titanium Dioxide by Nitrogen Doping. Japanese Journal of Applied Physics, 2001, 40, L561-L563.	1.5	541
3	Selective CO ₂ Conversion to Formate Conjugated with H ₂ O Oxidation Utilizing Semiconductor/Complex Hybrid Photocatalysts. Journal of the American Chemical Society, 2011, 133, 15240-15243.	13.7	458
4	Visibleâ€Lightâ€Induced Selective CO ₂ Reduction Utilizing a Ruthenium Complex Electrocatalyst Linked to a pâ€Type Nitrogenâ€Doped Ta ₂ O ₅ Semiconductor. Angewandte Chemie - International Edition, 2010, 49, 5101-5105.	13.8	325
5	A Highly Efficient Mononuclear Iridium Complex Photocatalyst for CO ₂ Reduction under Visible Light. Angewandte Chemie - International Edition, 2013, 52, 988-992.	13.8	277
6	Solar CO2 reduction using H2O by a semiconductor/metal-complex hybrid photocatalyst: enhanced efficiency and demonstration of a wireless system using SrTiO3 photoanodes. Energy and Environmental Science, 2013, 6, 1274.	30.8	251
7	Nitrogen complex species and its chemical nature in TiO2 for visible-light sensitized photocatalysis. Chemical Physics, 2007, 339, 57-63.	1.9	214
8	Deep-level optical spectroscopy investigation of N-doped TiO2 films. Applied Physics Letters, 2005, 86, 132104.	3.3	191
9	Photoelectrochemical reduction of CO2 in water under visible-light irradiation by a p-type InP photocathode modified with an electropolymerized ruthenium complex. Chemical Communications, 2010, 46, 6944.	4.1	180
10	A monolithic device for CO ₂ photoreduction to generate liquid organic substances in a single-compartment reactor. Energy and Environmental Science, 2015, 8, 1998-2002.	30.8	157
11	Optical bandgap widening of p-type Cu2O films by nitrogen doping. Applied Physics Letters, 2009, 94, .	3.3	156
12	Synthesis and Optical Properties of Monolayer Organosilicon Nanosheets. Journal of the American Chemical Society, 2010, 132, 5946-5947.	13.7	154
13	Photoelectrochemical CO ₂ reduction using a Ru(<scp>ii</scp>)–Re(<scp>i</scp>) multinuclear metal complex on a p-type semiconducting NiO electrode. Chemical Communications, 2015, 51, 10722-10725.	4.1	131
14	Selective CO2 conversion to formate in water using a CZTS photocathode modified with a ruthenium complex polymer. Chemical Communications, 2011, 47, 12664.	4.1	127
15	Enhanced photocatalytic activity of TiO2â^'xNx loaded with copper ions under visible light irradiation. Applied Catalysis A: General, 2006, 314, 123-127.	4.3	126
16	Photodegradation of toluene over TiO2–xNx under visible light irradiation. Physical Chemistry Chemical Physics, 2006, 8, 1116.	2.8	120
17	Photocatalytic Oxidation of NOx under Visible LED Light Irradiation over Nitrogen-Doped Titania Particles with Iron or Platinum Loading. Journal of Physical Chemistry C, 2008, 112, 12425-12431.	3.1	119
18	Toward Solar-Driven Photocatalytic CO ₂ Reduction Using Water as an Electron Donor. Inorganic Chemistry, 2015, 54, 5105-5113.	4.0	115

#	Article	IF	CITATIONS
19	Visible-light-induced photocatalytic oxidation of carboxylic acids and aldehydes over N-doped TiO2 loaded with Fe, Cu or Pt. Applied Catalysis B: Environmental, 2008, 83, 56-62.	20.2	110
20	Solar-Driven Photocatalytic CO ₂ Reduction in Water Utilizing a Ruthenium Complex Catalyst on p-Type Fe ₂ O ₃ with a Multiheterojunction. ACS Catalysis, 2018, 8, 1405-1416.	11.2	110
21	Direct assembly synthesis of metal complex–semiconductor hybrid photocatalysts anchored by phosphonate for highly efficient CO2 reduction. Chemical Communications, 2011, 47, 8673.	4.1	108
22	Electrical characterization of p-type N-doped ZnO films prepared by thermal oxidation of sputtered Zn3N2 films. Applied Physics Letters, 2006, 88, 172103.	3.3	105
23	Charge Separation and Trapping in N-Doped TiO ₂ Photocatalysts: A Time-Resolved Microwave Conductivity Study. Journal of Physical Chemistry Letters, 2010, 1, 3261-3265.	4.6	103
24	Photocatalytic CO ₂ Reduction Using a Robust Multifunctional Iridium Complex toward the Selective Formation of Formic Acid. Journal of the American Chemical Society, 2020, 142, 10261-10266.	13.7	90
25	Low-Energy Electrocatalytic CO ₂ Reduction in Water over Mn-Complex Catalyst Electrode Aided by a Nanocarbon Support and K ⁺ Cations. ACS Catalysis, 2018, 8, 4452-4458.	11.2	79
26	Electrical characterization of band gap states in C-doped TiO2 films. Applied Physics Letters, 2005, 87, 052111.	3.3	68
27	Visible light-sensitive mesoporous N-doped Ta2O5 spheres: synthesis and photocatalytic activity for hydrogen evolution and CO2 reduction. Journal of Materials Chemistry, 2012, 22, 24584.	6.7	65
28	Structural Improvement of CaFe ₂ O ₄ by Metal Doping toward Enhanced Cathodic Photocurrent. ACS Applied Materials & Interfaces, 2014, 6, 10969-10973.	8.0	65
29	Z-scheme water splitting under visible light irradiation over powdered metal-complex/semiconductor hybrid photocatalysts mediated by reduced graphene oxide. Journal of Materials Chemistry A, 2015, 3, 13283-13290.	10.3	65
30	Origin of visible-light sensitivity in N-doped TiO2 films. Chemical Physics, 2007, 339, 20-26.	1.9	58
31	Photoinduced Electron Transfer from Nitrogen-Doped Tantalum Oxide to Adsorbed Ruthenium Complex. Journal of Physical Chemistry C, 2011, 115, 18348-18353.	3.1	58
32	Charge-Carrier Dynamics in Nitrogen-Doped TiO ₂ Powder Studied by Femtosecond Time-Resolved Diffuse Reflectance Spectroscopy. Journal of Physical Chemistry C, 2012, 116, 1286-1292.	3.1	58
33	Dual functional modification by N doping of Ta2O5: p-type conduction in visible-light-activated N-doped Ta2O5. Applied Physics Letters, 2010, 96, .	3.3	56
34	Photocatalytic CO ₂ Reduction Using Water as an Electron Donor under Visible Light Irradiation by Z-Scheme and Photoelectrochemical Systems over (CuGa) _{0.5} ZnS ₂ in the Presence of Basic Additives. Journal of the American Chemical Society, 2022, 144, 2323-2332.	13.7	56
35	Enhancement of CO2 reduction activity under visible light irradiation over Zn-based metal sulfides by combination with Ru-complex catalysts. Applied Catalysis B: Environmental, 2018, 224, 572-578.	20.2	55
36	A large-sized cell for solar-driven CO2 conversion with a solar-to-formate conversion efficiency of 7.2%. Joule, 2021, 5, 687-705.	24.0	54

#	Article	IF	CITATIONS
37	Z-Schematic and visible-light-driven CO ₂ reduction using H ₂ O as an electron donor by a particulate mixture of a Ru-complex/(CuGa) _{1â^x} Zn _{2x} S ₂ hybrid catalyst, BiVO ₄ and an electron mediator. Chemical Communications, 2018, 54, 10199-10202.	4.1	52
38	Photoelectrochemical hydrogen production by water splitting over dual-functionally modified oxide: p-Type N-doped Ta2O5 photocathode active under visible light irradiation. Applied Catalysis B: Environmental, 2017, 202, 597-604.	20.2	49
39	Solar-Driven CO ₂ Reduction Using a Semiconductor/Molecule Hybrid Photosystem: From Photocatalysts to a Monolithic Artificial Leaf. Accounts of Chemical Research, 2022, 55, 933-943.	15.6	47
40	Self-assembled Cuprous Coordination Polymer as a Catalyst for CO ₂ Electrochemical Reduction into C ₂ Products. ACS Catalysis, 2020, 10, 10412-10419.	11.2	44
41	Charge-Carrier Dynamics in Cu- or Fe-Loaded Nitrogen-Doped TiO ₂ Powder Studied by Femtosecond Diffuse Reflectance Spectroscopy. Journal of Physical Chemistry C, 2013, 117, 16448-16456.	3.1	42
42	Highly crystalline β-FeOOH(Cl) nanorod catalysts doped with transition metals for efficient water oxidation. Sustainable Energy and Fuels, 2017, 1, 636-643.	4.9	40
43	Remarkably enhanced photocatalytic activity by nickel nanoparticle deposition on sulfur-doped titanium dioxide thin film. Applied Catalysis B: Environmental, 2009, 87, 239-244.	20.2	37
44	p -type conduction induced by N-doping in Î \pm -Fe2O3. Applied Physics Letters, 2011, 98, .	3.3	37
45	Deep-level characterization of N-doped ZnO films prepared by reactive magnetron sputtering. Applied Physics Letters, 2005, 87, 232104.	3.3	35
46	Stoichiometric water splitting using a p-type Fe ₂ O ₃ based photocathode with the aid of a multi-heterojunction. Journal of Materials Chemistry A, 2017, 5, 6483-6493.	10.3	34
47	Solar-driven CO ₂ to CO reduction utilizing H ₂ O as an electron donor by earth-abundant Mn–bipyridine complex and Ni-modified Fe-oxyhydroxide catalysts activated in a single-compartment reactor. Chemical Communications, 2019, 55, 237-240.	4.1	33
48	[Ir(tpy)(bpy)Cl] as a Photocatalyst for CO ₂ Reduction under Visibleâ€Light Irradiation. ChemPhotoChem, 2018, 2, 207-212.	3.0	32
49	Sodium hexatitanate photocatalysts prepared by a flux method for reduction of carbon dioxide with water. Catalysis Today, 2018, 303, 296-304.	4.4	26
50	Molecular Catalysts Immobilized on Semiconductor Photosensitizers for Proton Reduction toward Visibleâ€Lightâ€Driven Overall Water Splitting. ChemSusChem, 2019, 12, 1807-1824.	6.8	25
51	Highly Enhanced Electrochemical Water Oxidation Reaction over Hyperfine β-FeOOH(Cl):Ni Nanorod Electrode by Modification with Amorphous Ni(OH)2. Bulletin of the Chemical Society of Japan, 2018, 91, 778-786.	3.2	24
52	Photoelectrochemical water-splitting over a surface modified p-type Cr ₂ O ₃ photocathode. Dalton Transactions, 2020, 49, 659-666.	3.3	23
53	Photocatalytic Degradation of Formaldehyde and Toluene Mixtures in Air with a Nitrogen-doped TiO2Photocatalyst. Chemistry Letters, 2006, 35, 616-617.	1.3	20
54	Electrocatalytic CO ₂ reduction near the theoretical potential in water using Ru complex supported on carbon nanotubes. Nanotechnology, 2018, 29, 034001.	2.6	19

#	Article	IF	CITATIONS
55	Solar Fuel Production from CO ₂ Using a 1 m-Square-Sized Reactor with a Solar-to-Formate Conversion Efficiency of 10.5%. ACS Sustainable Chemistry and Engineering, 2021, 9, 16031-16037.	6.7	18
56	Nitrogen and transition-metal codoped titania nanotube arrays for visible-light-sensitive photoelectrochemical water oxidation. Chemical Communications, 2014, 50, 7614.	4.1	17
57	First principles calculations of surface dependent electronic structures: a study on \hat{I}^2 -FeOOH and \hat{I}^3 -FeOOH. Physical Chemistry Chemical Physics, 2019, 21, 18486-18494.	2.8	17
58	Materials design and development of functional materials for industry. Journal of Physics Condensed Matter, 2008, 20, 064227.	1.8	15
59	Photoactivity of p-Type α-Fe ₂ O ₃ Induced by Anionic/Cationic Codoping of N and Zn. Applied Physics Express, 2013, 6, 041201.	2.4	14
60	Electrochemical Water Oxidation Catalysed by CoOâ€Co ₂ O ₃ â€Co(OH) ₂ Multiphaseâ€Nanoparticles Prepared by Femtosecond Laser Ablation in Water. ChemistrySelect, 2018, 3, 4979-4984.	1.5	14
61	Band bending and dipole effect at interface of metal-nanoparticles and TiO ₂ directly observed by angular-resolved hard X-ray photoemission spectroscopy. Physical Chemistry Chemical Physics, 2018, 20, 11342-11346.	2.8	12
62	Effects of Ta ₂ O ₅ Surface Modification by NH ₃ on the Electronic Structure of a Ru-Complex/N–Ta ₂ O ₅ Hybrid Photocatalyst for Selective CO ₂ Reduction. Journal of Physical Chemistry C, 2018, 122, 1921-1929.	3.1	12
63	Low-Overpotential Electrochemical Water Oxidation Catalyzed by CuO Derived from 2 nm-Sized Cu ₂ (NO ₃)(OH) ₃ Nanoparticles Generated by Laser Ablation at the Air–Liquid Interface. ACS Applied Energy Materials, 2020, 3, 8383-8392.	5.1	12
64	Operando X-ray absorption spectroscopy of hyperfine β-FeOOH nanorods modified with amorphous Ni(OH)2 under electrocatalytic water oxidation conditions. Chemical Communications, 2020, 56, 5158-5161.	4.1	12
65	Self-Assembled Single-Crystalline GaN Having a Bimodal Meso/Macropore Structure To Enhance Photoabsorption and Photocatalytic Reactions. ACS Applied Materials & Interfaces, 2019, 11, 4233-4241.	8.0	11
66	Evaluation of photocatalytic activities and characteristics of Cu- or Fe-modified nitrogen-doped titanium dioxides for applications in environmental purification. Japanese Journal of Applied Physics, 2016, 55, 01AA05.	1.5	10
67	Electrochemical CO ₂ reduction over nanoparticles derived from an oxidized Cu–Ni intermetallic alloy. Chemical Communications, 2020, 56, 15008-15011.	4.1	10
68	Trap levels in tris(8-hydroxyquinoline) aluminum studied by deep-level optical spectroscopy. Applied Physics Letters, 2006, 88, 252104.	3.3	8
69	Carbon microfiber layer as noble metal-catalyst support for selective CO2 photoconversion in phosphate solution: Toward artificial photosynthesis in a single-compartment reactor. Journal of Photochemistry and Photobiology A: Chemistry, 2016, 327, 1-5.	3.9	8
70	Spectrally robust series/parallel-connected triple-junction photovoltaic cells used for artificial photosynthesis. Journal of Applied Physics, 2020, 127, .	2.5	8
71	A Highly Durable, Self-Photosensitized Mononuclear Ruthenium Catalyst for CO2 Reduction. Synlett, 2022, 33, 1137-1141.	1.8	8
72	Photocatalytic CO2 reduction by a Z-scheme mechanism in an aqueous suspension of particulate (CuGa)0.3Zn1.4S2, BiVO4 and a Co complex operating dual-functionally as an electron mediator and as a cocatalyst. Applied Catalysis B: Environmental, 2022, 316, 121600.	20.2	8

#	Article	IF	CITATIONS
73	Photocatalytic CO ₂ Reduction Using an Iron–Bipyridyl Complex Supported by Two Phosphines for Improving Catalyst Durability. Organometallics, 2022, 41, 1865-1871.	2.3	7
74	Deep-Level Characterization of Tris(8-hydroxyquinoline) Aluminum with and without Quinacridone Doping. Japanese Journal of Applied Physics, 2007, 46, 2636-2639.	1.5	6
75	Emissive Interface States in Organic Light-Emitting Diodes Based on Tris(8-hydroxyquinoline) Aluminum. Japanese Journal of Applied Physics, 2008, 47, 464-467.	1.5	6
76	High-pressure synthesis of ε-FeOOH from β-FeOOH and its application to the water oxidation catalyst. RSC Advances, 2020, 10, 44756-44767.	3.6	6
77	Electrochemical CO2 reduction improved by tuning the Cu-Cu distance in halogen-bridged dinuclear cuprous coordination polymers. Journal of Catalysis, 2021, 404, 12-17.	6.2	5
78	CO2 Reduction by Photoelectrochemistry. Lecture Notes in Energy, 2016, , 281-296.	0.3	4
79	Formation of C2 organic molecules from CO ₂ and H ₂ O by femtosecond laser induced chemical reactions in water. Japanese Journal of Applied Physics, 2020, 59, 057001.	1.5	4
80	Study of Excited States and Electron Transfer of Semiconductorâ€Metalâ€Complex Hybrid Photocatalysts for CO 2 Reduction by Using Picosecond Timeâ€Resolved Spectroscopies. Chemistry - A European Journal, 2021, 27, 1127-1137.	3.3	4
81	Aminoalkylsilane-modified Silver Cathodes for Electrochemical CO ₂ Reduction. Chemistry Letters, 2016, 45, 1362-1364.	1.3	3
82	Charge Trapping Process in Photoexcited Nitrogen-Doped Titanium Oxides. Inorganic Chemistry, 2020, 59, 10439-10449.	4.0	3
83	Carbon Nanohorn Support for Solar driven CO ₂ Reduction to CO Catalyzed by Mnâ€complex in an All Earthâ€abundant System. ChemNanoMat, 2021, 7, 596-599.	2.8	3
84	Light-Driven Carbon Dioxide Reduction Devices. Green Chemistry and Sustainable Technology, 2018, , 259-280.	0.7	2
85	Particulate photocatalytic reactors with spectrum-splitting function for artificial photosynthesis. Physical Chemistry Chemical Physics, 2021, 23, 15659-15674.	2.8	2
86	Hot-carrier photocatalysts for artificial photosynthesis. Journal of Chemical Physics, 2022, 156, 164705.	3.0	1
87	Deep-Level Optical Spectroscopy Investigation of Trap Levels in Tris(8-Hydroxyquinoline) Aluminum. Materials Research Society Symposia Proceedings, 2006, 965, 1.	0.1	0
88	Electrochemical CO ₂ Reduction to HCOOH Catalyzed by Ag <i>_n</i> (NO ₃) <i>_n</i> ₊₁ Clusters Prepared by Laser Ablation at the Air-Liquid Interface. Chemistry Letters, 2021, 50, 1941-1944.	1.3	0